MADRID 2015
1-4 June 2015 | IFEMA Madrid

Th N103 10

Joint 3D Source-side Deghosting and Designature for Modern Air-gun Arrays

P. Wang (CGG), K. Nimsaila* (CGG), D. Zhuang (CGG), Z. Fu (CGG), H. Shen (CGG), G. Poole (CGG) & N. Chazalnoel (CGG)

SUMMARY

Receiver deghosting has been widely used to extend the bandwidth of marine seismic data. Efforts have also been made to remove the source ghost and signature to further maximize the bandwidth of the acquired seismic data. We present an inversion scheme for angle-dependent source deghosting and designature that honours modern complex air-gun array geometry. Using both a synthetic ocean bottom node data set and a field streamer data set acquired with a multi-level source, we demonstrate that our method effectively removes source ghost and signature either separately or jointly. The resulting images have a wider bandwidth.

Introduction

One tactic for extending the bandwidth of marine seismic data starts with the removal of the receiver-side ghost. To further maximize the bandwidth of the acquired seismic data, complementary efforts have been made to remove the source-side ghost and signature. A common practice is to apply a single 1D filter (zero-angle approximation) to remove the source-side ghost and/or signature (Ziolkowski et al. 1982; Amundsen 1993). Angle-dependent designature methods have been proposed since the 1980s (Van der Schans et al. 1983; Poole et al. 2013). Several recent developments use receiver deghosting algorithms (Riyanti et al. 2008; Wang et al. 2013, 2014; Poole 2013) to approximate source deghosting. Those methods often assume a single point source for source deghosting, which renders them less effective for modern complex air-gun array geometry such as the multi-level air-gun array (Siliqi et al. 2013). We propose an algorithm for angle-dependent source deghosting and designature that takes into account the effect of air-gun array geometry.

Method

Sparse 3D Tau-P inversion has been proposed for 3D deghosting of marine seismic data (Wang et al. 2014). The key is to invert for ghost-free data, U, which when reghosted and inverse Tau-P transformed equals the input data, D:

$$D(f;x_0^i,y_0^i)=\sum_j L(f;x_0^i,y_0^i;p_x^j,p_y^j)R(f;z_0^i;p_x^j,p_y^j)U(f;p_x^j,p_y^j), \quad (1)$$

where f is frequency, L is the reverse Tau-P transform operator, R is the reghosting operator, (x_0^i,y_0^i,z_0^i) is the average air-gun array location, and (p_x^j,p_y^j) is the slowness pair (i: trace index; j: slowness index). Most, if not all, deghosting methods when being used for source deghosting assume a single point source. To handle the source ghost and signature for complex air-gun arrays, we extended this algorithm by replacing R with the following air-gun array term, G:

$$G(f;x_0^i,y_0^i,z_0^i;p_x^j,p_y^j)=\sum_k R_k^{ij}(f;z_k^i;p_x^j,p_y^j)S_k^{ij}(f;x_k^i,y_k^i,z_k^i;p_x^j,p_y^j), \quad (2)$$

where R_k^{ij} is the reghosting operator, S_k^{ij} is the resignature operator, and (x_k^i,y_k^i,z_k^i) represents the location of the k^{th} notional source. The reghosting operator, R_k^{ij}, and resignature operator, S_k^{ij}, can be written as

$$R_k^{ij}=e^{-i2\pi f z_k^i\sqrt{v^{-2}-(p_x^j)^2-(p_y^j)^2}}-e^{i2\pi f z_k^i\sqrt{v^{-2}-(p_x^j)^2-(p_y^j)^2}} \text{ and}$$
$$S_k^{ij}=S_k^0(f)e^{-i2\pi f\left[t_k^0+(x_k^i-x_0^i)p_x+(y_k^i-y_0^i)p_y+(z_k^i-z_0^i)\sqrt{v^{-2}-\left(p_x^j\right)^2-\left(p_y^j\right)^2}\right]}, \quad (3)$$

where v is the water velocity, S_k^0 is the notional source often obtained from near-field hydrophone measurements (Ziolkowski et al. 1982; Poole et al. 2013), and t_k^0 is the notional source delay-time used to synchronize individual notional sources (Siliqi et al. 2013). By substituting Equation 3 into Equation 2 and then replacing R in Equation 1 with G, we formulated an inverse problem that performs joint source deghosting and designature to invert for ghost- and signature-free data, U:

$$D(f;x_0^i,y_0^i)=\sum_j L(f;x_0^i,y_0^i;p_x^j,p_y^j)(\sum_k R_k^{ij}S_k^{ij})U(f;p_x^j,p_y^j). \quad (4)$$

We can drop R_k^{ij} from Equation 4 to perform source designature only. If source designature (debubbling) has already been applied, and only source deghosting is required, the notional source, S_k^{ij}, may be replaced with spikes proportional to the amplitude emitted from each gun.

Application to ocean bottom node data

We applied this algorithm to a synthetic ocean bottom node (OBN) data set for joint source deghosting and designature. We used an air-gun array consisting of 32 notional sources (Figure 1). The notional

sources came from near-field hydrophone measurements of a real survey. The OBN node is at 500 m depth, and the surface offsets are 1000 m.

Each synthetic trace shown in Figure 2a corresponds to a shot location on the blue circle (Figure 1) with the first trace at 0° azimuth and the last trace at 360° azimuth. The wavelet is sharper at 0°/180° azimuth than that at 90°/270° azimuth. We also observed more high-frequency amplitude loss at 90°/270° azimuth than at 0°/180° azimuth (Figures 2c-2f, blue lines). This directional wavelet variation is also typical for real-world OBN data. After the joint source deghosting and designature method, the ghost and signature (bubble) are effectively removed, and the azimuthal wavelet variation is normalized (Figure 2b). Figures 2c-2f compare amplitude spectra before/after joint source deghosting and designature for azimuthal angles of 0°, 90°, 180°, and 270°, respectively. The blue lines show the amplitude spectra of the input data before source deghosting and designature. The oscillation at the low-frequency end of the spectrum corresponds to bubbles, the low frequency loss is due to the source ghost, and the different levels of high-frequency drops are due to the air-gun array directivity. The red lines represent the amplitude spectra after joint source deghosting and designature. The low-frequency source-ghost notch is properly filled in, the bubble is removed, and more importantly, the high-frequency content is equalized for different azimuthal angles. This may be important for 4D time-lapse processing.

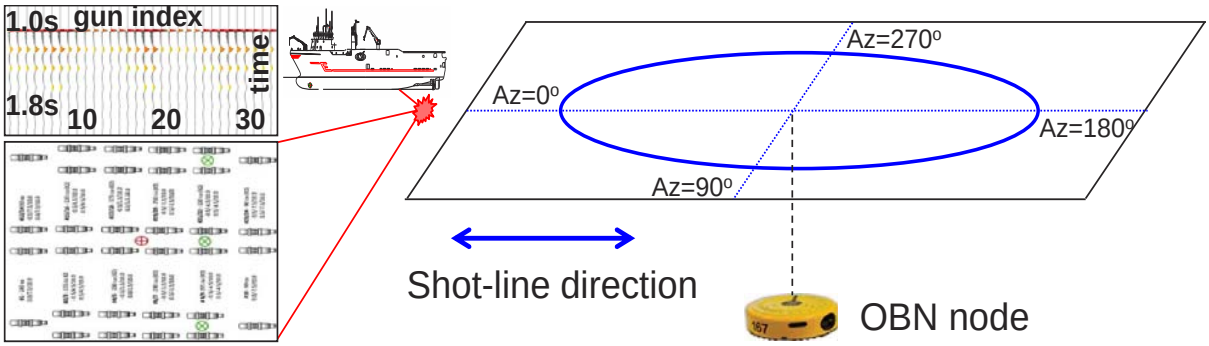

Figure 1 *OBN configuration for synthetic modelling. Bottom left: The air-gun array consisting of 32 notional sources. Top left: The source signature for each notional source. The OBN sits on the water bottom at 500 m depth. The blue circle indicates the shot locations with a surface offset of 1000 m and azimuthal angles ranging from 0° to 360°. The shot-line direction corresponds to 0°-180° azimuth.*

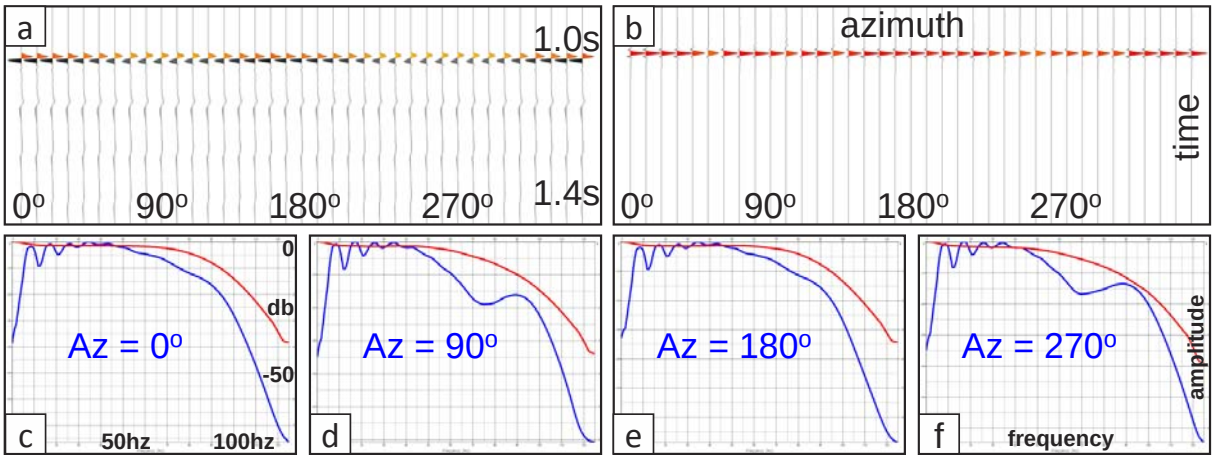

Figure 2 *(a) Synthetic data before joint source deghosting and designature. There are 37 traces corresponding to azimuthal angles of 0° to 360° with a 10° interval. (b) Data after joint source deghosting and designature. (c)-(f) The amplitude spectra before (blue) and after (red) joint source deghosting and designature for azimuthal angles of 0°, 90°, 180°, and 270°, respectively.*

Application to multi-level source streamer data

We tested our algorithm for source deghosting (note: the input data were after receiver deghosting, and a 1D designature filter was applied before that) on multi-level source streamer data from offshore West Africa acquired with variable-depth streamers towed at depths from 8 m to 50 m (Soubaras 2010). The air-gun array consisted of 21 notional sources positioned at different depths of 6 m and 9 m. The 9 m notional sources fired 2 ms after the 6 m notional sources so that the source-side down-going wavefields (primary) of the deeper notional sources was synchronized with the source-side down-going wavefields of the shallower notional sources (by zero-angle approximation). Meanwhile, the source-side up-going wavefields (source ghost) did not coincide with one another (Siliqi et al. 2013). For this reason, the amplitude of the primary (Figure 3a, black wavelet) is higher than that of the ghost (Figure 3a, white wavelet). Another key feature of this acquisition is that there are no apparent source-ghost notches on the amplitude spectrum (Figure 3f, red line) because the 6 m source-ghost peaks were complementary to the 9 m source-ghost notches, although the ghost wavelet and residual ghost notches may still be observed.

The colored lines in Figure 3a show the ray paths of the water bottom events: 6 m primary (Figure 3b), 9 m primary (Figure 3c), 6 m source ghost (Figure 3d), and 9 m source ghost (Figure 3e). The input common-offset section was decomposed into four similar wavefields using our method. We kept all four components at their own timing and polarity in Figures 3b-e (i.e., we could add them together to recover the input data). For the final deghosted output, we re-datumed the primaries from different gun depths to

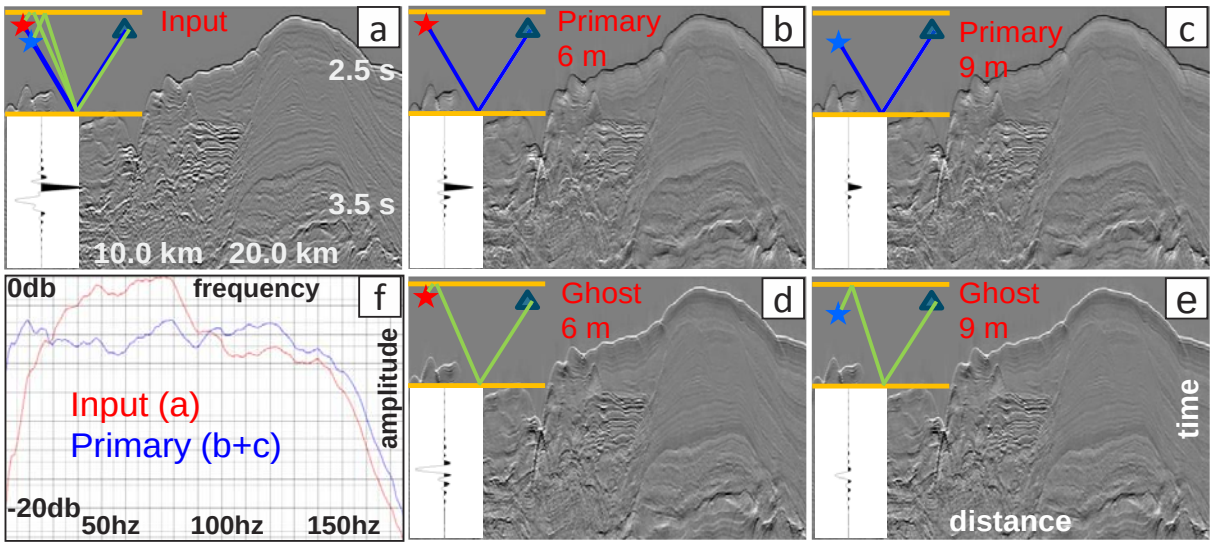

Figure 3 *(a) Input data before source deghosting. Primary for (b) 6 m notional sources and (c) 9 m notional sources. Ghost for (d) 6 m notional sources and (e) 9 m notional sources. (f) Spectral comparison between input data (red) and total primaries (blue).*

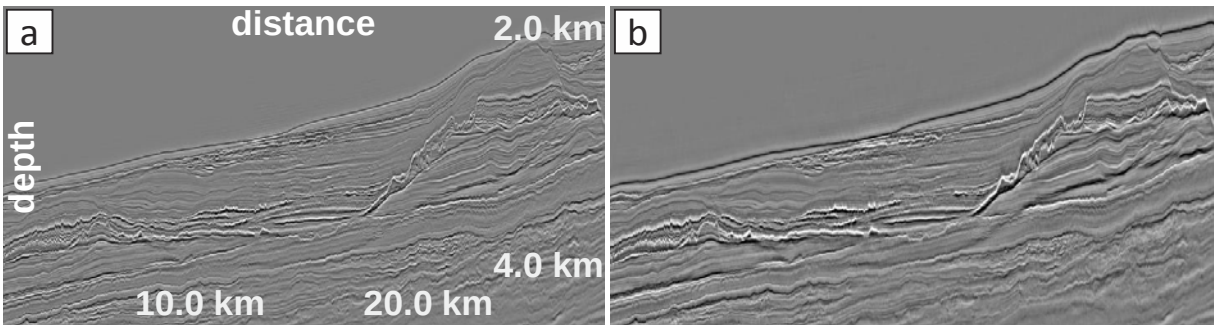

Figure 4 *Stacked Kirchhoff migration images for data (a) after receiver deghosting and (b) followed by the proposed source deghosting.*

the water surface and then summed them together. By doing this, we synchronized the primaries from all the notional sources for all propagation angles (vs. the survey synchronization that is only good at zero angles). Figure 3f shows the spectral comparison of the input data and the final deghosted output (total primaries from all the notional sources). The data after source deghosting have a wider bandwidth. The zero-frequency source-ghost notch is properly filled in, and the residual source-ghost notches due to 6 m and 9 m notional sources are compensated. Figure 4 compares the stacked Kirchhoff migration images after receiver deghosting (4a) and followed by the proposed source deghosting (4b). We observed that our source deghosting further sharpens the image.

Discussion and Conclusions

We proposed a source deghosting and designature inversion scheme to compensate for 3D source-side ghost and signature for both OBN and streamer data. We demonstrated that source deghosting and/or designature produces a sharper wavelet and wider bandwidth that can be beneficial for seismic interpretation and reservoir characterization.

Theoretically, this method requires the input data in the common-receiver domain, which is inherently natural for OBN geometry that has stationary receivers. For streamer data, common-receiver gathers can only be approximated due to non-stationary receivers, and they are usually not dense enough because of coarse shot sampling perpendicular to the shooting direction. A practical solution is to use shot gathers as the input. The underlying assumption is that surface incidence angles on the source side are the same as (or close to) those on the receiver side. This can introduce inaccuracies for complex subsurface geology. However, we found that source deghosting and/or designature using shot gathers as input works better than a 1D deghosting/designature filter, which assumes surface incidence angles of 0^o.

Acknowledgements

We thank Xu Li for testing of the algorithm. We also thank CGG for permission to publish this work. Special thanks go to Jerry Young for support and constructive discussions

References

Amundsen, L. [1993] Estimation of source array signatures. *Geophysics*, **58**, 1865-1869.
Poole, G., Davison, C., Deeds, J., Davies, K. and Hampson, G. [2013] Shot-to-shot directional designature using near-field hydrophone data. *83rd SEG Annual International Meeting*, Expanded Abstracts, 4236-4240.
Poole, G., [2013] Premigration receiver deghosting and redatuming for variable depth streamer data. *83rd SEG Annual International Meeting*, Expanded Abstracts.
Riyanti, C., van Borselen, R., van den Bert, P. and Fokkema, J. [2008] Pressure wave-field deghosting for non-horizontal streamers. *78th SEG Annual International Meeting*, Expanded Abstracts, 2652-2656.
Soubaras, R. [2010] Variable-depth streamer: deep towing and efficient deghosting for extended band-width. SEG/EAGE Research workshop.
Siliqi, R., Payen T., Sablon R. and Desrues K. [2013] Synchronized multilevel source, a robust broadband marine solution. *83rd SEG Annual International Meeting*, Expanded Abstracts.
Van der Schans, C. A. and Ziolkowski, A.M. [1983] Angular-dependent signature deconvolution. *53rd SEG Annual International Meeting*, Expanded Abstracts, 433-435.
Wang, P., Ray S., Peng C., Li Y. and Poole G. [2013] Premigration deghosting for marine streamer data using a bootstrap approach in tau-p domain. *75th EAGE Conference & Exhibition*, Extended Abstracts, 4221-4225.
Wang, P., Ray, S. and Nimsaila, K. [2014] 3D joint deghost and crossline interpolation for marine single-component streamer data. *84th SEG Annual International Meeting*, Expanded Abstracts, 3594-3598.
Ziolkowski, A., Parkes, G.E., Hatton, L. and Haughland, T. [1982] The signature of an air gun array: Computation from near-field measurements including interactions. *Geophysics*, **47**, 1413-1421.